# Deep Inelastic Neutron Scattering Studies of Atomic Momentum Distributions in Condensed Argon and Neon[†, *]

M. A. Fradkin, S.-X. Zeng, and R. O. Simmons

Physics Department and Materials Research Laboratory, University of Illinois at Urbana-Champaign, USA

Z. Naturforsch. **48a**, 438–442 (1993); received December 23, 1991

Using deep inelastic neutron scattering, direct measurements have been made, i) of the dynamic structure factor of a series of condensed argon samples over the temperature range 18 to 85 K, near melting (for wave-vector transfers 12 to 26 $Å^{-1}$) and ii) of liquid neon, near 27 K (for wave-vector transfers 10.4 to 27.6 $Å^{-1}$). Neutron time-of-flight chopper spectrometers were employed. Single-particle kinetic energies, $\langle E_k \rangle$, can be obtained from the analysis of the Doppler-broadened recoil spectrum of the target particles. For argon the temperature dependence of $\langle E_k \rangle$ can be compared to expectations from theory, from thermodynamic data, and from previous neutron scattering measurements on collective vibrational modes. For liquid neon the wave-vector-transfer dependence of $J(y)$, the longitudinal momentum distribution function, is being analyzed for final-state effects.

*Key words:* Inelastic neutron scattering; Momentum distributions.

PACS Scheme 61.12.Gz, 61.25.Bi, 63.20.Pw.

## 1. Purpose

Using epithermal neutrons, direct measurements of single-particle momentum distributions in condensed matter are possible through deep inelastic scattering. Quantities directly related to the single-particle momentum distribution, such as the average single-particle kinetic energy, $\langle E_k \rangle$, a part of the total energy hitherto inaccessible to direct measurement, can be determined.

The condensed noble gases provide a prototype family that exhibits ranges of behavior, such as quantum to classical, increasing importance of multibody interatomic interactions with increasing atomic number, and increasing lattice vibrational anharmonicity with decreasing mass. Determination of the single-particle kinetic energy provides information as to the importance of these behaviors.

† Supported by U.S. Department of Energy BES-Materials Sciences under contract No. DE-FG02-91ER45439.

* Presented at the Sagamore X Conference on Charge, Spin and Momentum Densities, Konstanz, Fed. Rep. of Germany, September 1–7, 1991.

Reprint requests to Prof. R. O. Simmons, Physics Department, University of Illinois, 1110 W. Green St., Urbana, IL 61801, USA.

## 2. Method

Pulsed neutron spallation facilities, such as the Argonne National Laboratory Intense Pulsed Neutron Source (IPNS), are capable of producing the large flux of epithermal neutrons necessary to carry out deep inelastic neutron scattering studies. Chopper spectrometers, in which the incident neutron energy selection is performed by a phased Fermi chopper and the final neutron energy is determined via time of flight, were employed in these measurements (Figure 1). The instruments LRMECS and HRMECS were used to take the argon data and neon data, respectively [1].

In the impulse approximation for neutron scattering, where the recoil of the target particle is assumed to be free, the dynamic structure factor $S_{IA}(\boldsymbol{Q}, E)$ is related to the atomic momentum distribution $n(\boldsymbol{p})$ simply by

$$S_{IA}(\boldsymbol{Q}, E) = \int n(\boldsymbol{p})\, \delta(E - E_r - \hbar \boldsymbol{Q} \cdot \boldsymbol{p}/M)\, \mathrm{d}\boldsymbol{p}\,, \qquad (1)$$

where $\boldsymbol{Q}$ is the wave-vector transfer, $E$ the energy transfer, $E_r$ the recoil energy of the target particle, and $M$ the atomic mass. The argument of the delta function expresses conservation of energy and momentum for the scattering process. For an isotropic Gaussian $n(\boldsymbol{p})$,

$$n(\boldsymbol{p}) = (\pi A)^{-3/2} \exp(-p^2/A)\,, \qquad (2)$$

0932-0784 / 93 / 0100-0438 $ 01.30/0. – Please order a reprint rather than making your own copy.

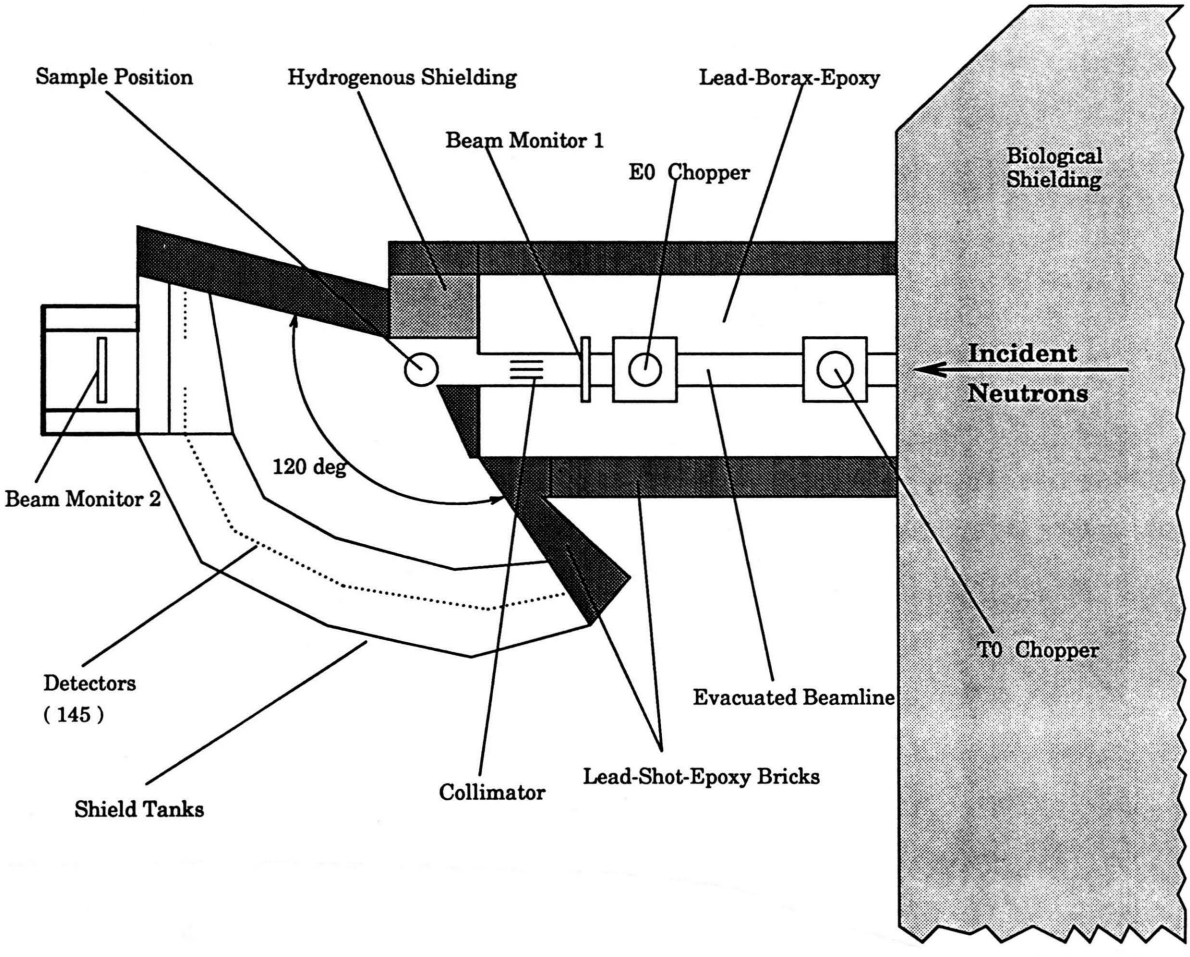


Fig. 1. Schematic horizontal section of the LRMECS spectrometer at IPNS-ANL [1]. Scattered neutrons can be detected over the broad angular range $-5°$ to $116°$.

where $A = 2MT^*$ and $T^*$ is an effective temperature, the dynamic structure factor assumes the Gaussian form,

$$S_{IA}(Q, E) = C \exp\{-(E - E_r)^2 M^2/(A\hbar^2 Q^2)\} . \quad (3)$$

$\langle E_k \rangle$ can be obtained by integration over all atomic momenta, weighted by the momentum distribution. $\langle E_k \rangle$ is related to $S_{IA}(Q, E)$ by

$$\langle E_k \rangle = (3/4)(A/M) . \quad (4)$$

Especially at large wave-vector transfers, inelastic neutron data are commonly presented in terms of $J(y)$, the longitudinal momentum distribution function, instead of $S(Q, E)$. For an isotropic system, $J(y)$ is related to $S(Q, E)$ by

$$J(y) = (\hbar Q/M) S(Q, E) , \quad (5)$$

where the scaling variable is

$$y = (M/\hbar^2 Q)(E - E_r) . \quad (6)$$

Various agents, such as instrument resolution, multiple scattering, and final-state effects (owing to the failure of the impulse approximation) can cause the observed $S(Q, E)$ spectrum to be non-Gaussian. The effects of these agents must be either reduced to a negligible level or accounted for in order to obtain accurate momentum distributions. For the data taken on condensed argon, multiple scattering and instrument resolution were accounted for by convoluting a Gaussian $J(y)$ with a fitting function. The fitting function was determined by fitting data from liquid argon samples, for which it is assumed that $\langle E_k \rangle$ is given by

the expansion [2]

$$\langle E_k \rangle = (3/2)\, k_B T \{1 + (1/12)(\Theta/T)^2 - (1/240)(\Theta/T)^4 + \ldots\}, \quad (7)$$

where

$$\Theta^2 = (\hbar^2/3 M k_B) \langle \Delta V \rangle . \quad (8)$$

From molecular-dynamics calculations for a Lennard-Jones liquid one can obtain, using the Lennard-Jones parameters of Rossi and Danon [3], a value of 615 K/Å$^2$ for the average value of the Laplacian of the potential energy for liquid argon at saturated vapor pressure at a temperature of 110.6 K [4].

We have assumed in our present analysis that our experimental conditions have satisfied the impulse approximation and hence that final-state effects are negligible. Justification for neglecting final-state effects in the case of liquid argon can be obtained from the theoretical work of Sears [5]. In Sears' treatment the measured $J(y)$ of an isotropic system is related to $J_{IA}(y)$ in the impulse approximation by

$$J(y) = J_{IA}(y) - A_3[d^3 J_{IA}(y)/dy^3] + A_4[d^4 J_{IA}(y)/dy^4] - \ldots , \quad (9)$$

where $J(y)$ is the measured longitudinal momentum distribution function, $J_{IA}(y)$ is the longitudinal momentum distribution function in the impulse approximation, and $A_3, A_4, \ldots$ are wave-vector-transfer dependent coefficients. All odd coefficients are antisymmetric in $Q$ and hence antisymmetric in $y$; all even coefficients are symmetric in $Q$ and symmetric in $y$. In particular, $A_3 = M\langle \Delta V \rangle / 36\hbar^2 Q$, where $V$ is the pair-potential energy and $M$ is the mass of the scatterer.

At $Q = 25$ Å$^{-1}$ we calculate for liquid argon at 110.6 K the first anti-symmetric term at its maximum to be approximately 1.5% of $J_{IA}(y)$ at that value of $y$. A correction of this size leaves the width, and hence $\langle E_k \rangle$, essentially unchanged from that of $J_{IA}(y)$. This can be seen in Fig. 2, in which we have plotted two curves, i) $J_{IA}(y)$, a Gaussian function having a width corresponding to an energy given by (7), and ii) the first antisymmetric term in the Sears expansion enlarged by a factor of 5 to aid visibility. Owing to the small size of the first antisymmetric term the expected measured $J(y)$, consisting of $J_{IA}(y)$ and the antisymmetric term, would not be visibly different from $J_{IA}(y)$ shown in Figure 2.

In solids, the magnitude of final-state effects is still uncertain, in part owing to the absence of realistic pair distribution functions and accompanying quantitative calculations of such effects. For present purposes of analysis we have assumed that final-state effects are negligible in our data on solid argon, which were taken at similar wave-vector transfers as our liquid-argon data.

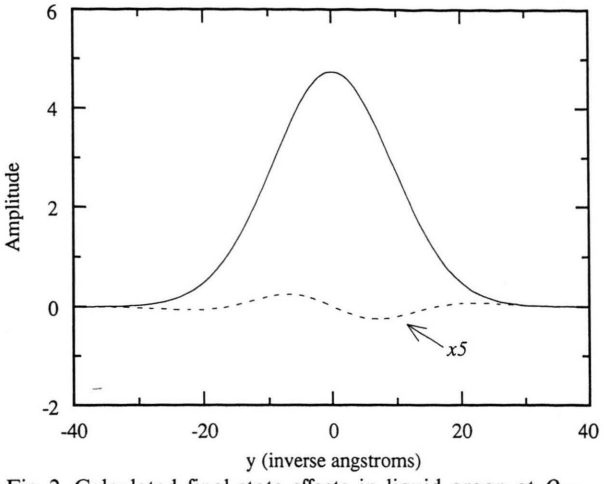


Fig. 2. Calculated final-state effects in liquid argon at $Q = 24$ Å$^{-1}$. The solid curve is $J_{IA}(y)$ for liquid argon at 110.6 K, taken to be a Gaussian function having a width corresponding to a single-particle kinetic energy of 112.7 K. The dashed curve is the first antisymmetric term in the Sears expansion, enlarged by a factor of 5 for visibility. Owing to the small size of the antisymmetric term the expected measured $J(y)$ is essentially the same as $J_{IA}(y)$.

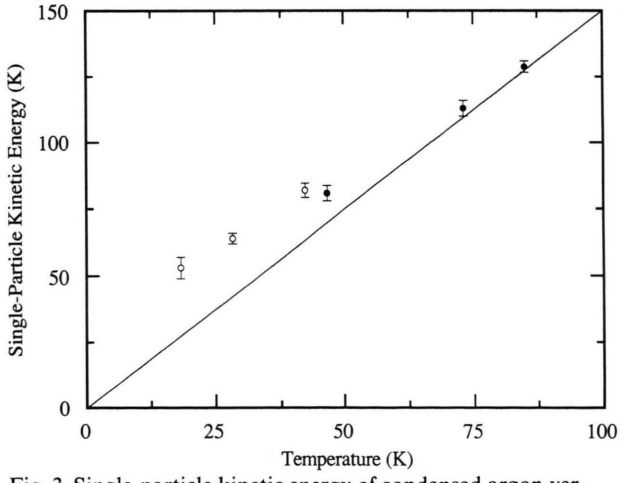


Fig. 3. Single-particle kinetic energy of condensed argon versus temperature. The solid line represents the value of $\langle E_k \rangle$ predicted by equipartition, (3/2) $k_B T$. Finite instrument resolution and multiple scattering have been accounted for using a fitting function derived from data on liquid argon. Liquid data taken at 110.6 K were used to determine the fitting function for the three low-temperature solid-argon data sets (open circles), liquid data taken at 87.4 K were used for the three high-temperature data sets (filled circles).

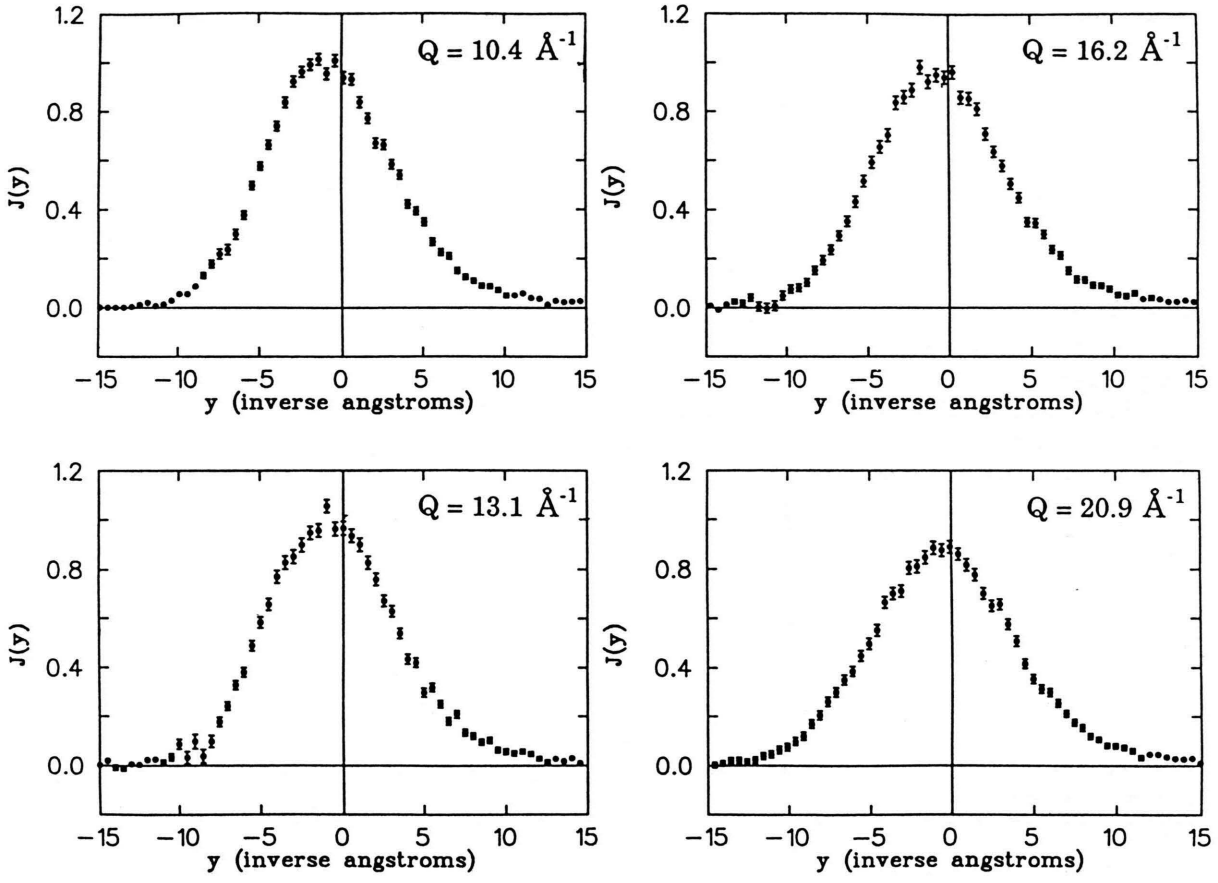


Fig. 4. Longitudinal momentum distribution function, $J(y)$, for liquid neon at approximately 27 K for four wave-vector transfers. These data were collected at a mean scattering angle of 87°, at incident neutron energies of 125, 195, 300, and 500 meV, respectively. They span a range of wave-vector transfers not previously explored, and it can been seen that the shape of $J(y)$ progressively changes. The explicit study of final-state effects in the scattering process is now possible.

## 3. Results for Condensed Argon

The temperature dependence of $\langle E_k \rangle$ for condensed argon shows a deviation from equipartition behavior at low temperatures (Figure 3). Several models, including the self-consistent-average-phonon model (SCAP) [6], are currently being investigated in order to account for the observed temperature dependence. Qualitatively the temperature dependence is that expected for a system of quantum oscillators. With an appropriate model it should be possible to deduce a value for the ground-state kinetic energy of solid argon. A Debye model employs the zero-temperature limit of the heat capacity, yielding $\langle E_k(T=0) \rangle = (9/16)\,\Theta_c(T=0) =$ 52 K, from a heat capacity $\Theta_c$ value of Finegold and Phillips [7].

## 4. Data on Liquid Neon

It is of interest to investigate more explicitly the domain of applicability of the impulse approximation. We have therefore undertaken to do this on fluid neon, an isotropic scattering system for which the Sears analysis [5] should apply. Prior to our study there was a wide gap in the available data. The measurements of Buyers et al. [8] had a maximum wave-vector transfer of 12.5 Å$^{-1}$ while those of Peek et al. [9] are for wave-vector transfer greater than 20 Å$^{-1}$. We studied a wide range of wave-vector transfers, 10.4 to 27.6 Å$^{-1}$, using the available range of scattering angles (87° to 136°) on the ANL spectrometer HRMECS [1] and different incident neutron energies.

Neon bridges the gap between the quantum behavior of condensed helium and the classical behavior of the heavier noble gas solids. It is therefore a good system for the study of final-state effects in the neutron–atom scattering process.

Shown in Fig. 4 is a subset of our data on fluid neon. From estimation of the value of $A_3$ (7) at $Q$ near 10 $Å^{-1}$ one expects to see a significant difference between $J(y)$ and $J_{IA}(y)$. Indeed, by comparison with the $J(y)$ data at larger $Q$ in Fig. 4, one sees, qualitatively, the expected change of shape, increased intensity at negative $y$ and reduced intensity at positive $y$. The data shown include the effects of finite instrument resolution and of multiple scattering, so further analysis is underway to refine this qualitative result.

*Acknowledgements*

This research has benefited from the use of the Intense Pulsed Neutron Source (IPNS) at Argonne Laboratory. This facility is funded by the U.S. Department of Energy, BES-Materials Sciences under contract No. W-31-109-ENG-38.

[1] C. K. Loong, S. Ikeda, and J. M. Carpenter, Nucl. Instrum. Methods A **260,** 381 (1987).
[2] V. F. Sears, Can. J. Phys. **63,** 68 (1985).
[3] J. C. Rossi and F. Danon, Discuss Faraday Soc. **40,** 97 (1965).
[4] L. Verlet, Phys. Rev. **159,** 98 (1967).
[5] V. F. Sears, Phys. Rev. B **30,** 44 (1984).
[6] K. Shukla, A. Paskin, D. O. Welch, and G. J. Dienes, Phys. Rev. B **24,** 724 (1981).
[7] L. Finegold and N. E. Phillips, Phys. Rev. **177,** 1383 (1969).
[8] W. J. L. Buyers, V. F. Sears, P. A. Lonngi, and D. A. Lonngi, Phys. Rev. A **11,** 697 (1975).
[9] D. A. Peek, M. C. Schmidt, I. Fujita, and R. O. Simmons, Phys. Rev. B **45,** 9671 (1992).